Peer-reviewed version available at Nanomaterials 2019, 9, 117; doi:10.3390/nano9010117

Article

ZIF-8 derived hollow carbon for efficient adsorption of antibiotics

Hongmei Tang,[a] Wenyao Li,[a,*] Haishun Jiang,[a] Runjia Lin,[b] Zhe Wang,[a] Jianghong Wu[c], Guanjie He[b,*] Paul R. Shearing[b] and Dan J. L. Brett[b,*]

[a] School of Materials Engineering, Shanghai University of Engineering Science, 333 Long Teng Road, Shanghai 201620, China
[b] Electrochemical Innovation Lab, Department of Chemical Engineering, University College London, London WC1E 7JE, UK
[c] College of Health Science and Environmental Engineering, Shenzhen Technology University, Shenzhen, Guangdong 518118, PR China.
* Corresponding authors, E-mail: liwenyao314@gmail.com, g.he@ucl.ac.uk, d.brett@ucl.ac.uk

Abstract: The harmful nature of high concentrations of antibiotics to humans and animals requires urgent development of novel materials and techniques for their absorption. In this work, CTAB (Cetyltrimethyl Ammonium Bromide)-assisted synthesis of ZIF-8 (zeolitic imidazolate framework) derived hollow carbon (ZHC) was designed, prepared and used as a high-performance adsorbent, further evaluated by Langmuir and Freundlich isothermal adsorption experiments, dynamic analysis as well as theoretical calculation. The maximum capacities of ZHC on adsorbing tetracycline (TC), norfloxacin (NFO) and levofloxacin (OFO) are 267.3, 125.6 and 227.8 mg g^{-1}, respectively, which delivers superior adsorptive performance when compared to widely studied inorganic adsorbates. The design concept of ZIFs-derived hollow carbon material provides guidance and insights for the efficient adsorbent of environmental antibiotics.

Keywords: ZIF-8; Hollow carbon; Antibiotics; Adsorbent

1. Introduction

Due to their outstanding medical properties, antibiotics are broadly utilized to treat infectious diseases; this leads to high-levels of antibiotics in hospital effluent and sewage treatment plants.[1] Since antibiotics cannot be easily metabolized by humans or animals, and it is inevitable to prevent the mass utilization of antibiotics, thus, a vicious cycle forms and result in the uncontrolled accumulation of residual antibiotics in the environment.[2] As known, antibiotics such as quinolones and tetracycline are able to make bacteria resistant to drugs and cause various diseases. Therefore, with the purpose of preventing the pollution of antibiotics, materials with tremendous absorption ability for antibiotics are urgently required.

In recent years, metal-organic frameworks (MOFs) have been synthesized *via* compounds composed of inorganic metal ions centers and organic ligands.[3] A great number of targeted applications can be achieved through the application of MOFs, owing to their diversity composed of various metal ions and organic ligands. Additionally, various morphologies of porous nanomaterials can be prepared by using MOFs as sacrificial templates through different thermal and/or chemical treatments. For instance, highly porous carbons can be produced *via* heat treatment of MOFs in an inert atmosphere, coupled with chemical etching for removal of the surface metal ions, thus leading to increased specific surface area. Compared with carbonaceous materials fabricated by conventional precursors, MOFs-derived carbons often exhibit controllable porous architectures, pore volumes and surface areas.[4] Various porous carbon materials, with controlled morphologies from 0 to 3-dimensions, have been successfully derived through carbonization of MOFs, highlighting their

versatility as precursors.[5-7] In addition to porous materials, MOF-derived carbons can be converted to hollow structures.

In this work, CTAB (Cetyltrimethyl Ammonium Bromide)-assisted synthesis of ZIF-8, a subclass of MOFs, was applied as a sacrificial template to synthesize ZIF hollow carbon (ZHC) nanostructures, with the aim of exploring highly efficient absorbent materials. The maximum adsorption capacities of ZHC for TC, NFO, and OFO are 267.3, 125.6, and 227.8 mg g^{-1}, respectively, according to the data obtained from Langmuir and Freundlich isothermal adsorption simulation as well as kinetic experiments. The adsorptive performance of ZHC is comparable to the cutting-edge inorganic adsorbents and paves a new way for the design concept of adsorbents.

2. Experimental

2.1. Chemicals

Zinc nitrate hexahydrate ($Zn(NO_3)_2 \cdot 6H_2O$), tannic acid (TA) and cetyltrimethylammonium bromide (CTAB, analytical purity) were all purchased from Sinopharm Chemical Reagent Co., Ltd. Anhydrous methanol (AR) and hydrochloric acid (HCl) were purchased from Shanghai Lingfeng Chemical Reagent Co., Ltd. 2-methylimidazole (AR 98%) was purchased from in Aladdin Industrial Corporation.

2.2. ZHC preparation

Firstly, 810 mg $Zn(NO_3)_2 \cdot 6H_2O$ were dissolved in 40 mL of anhydrous methanol solution with continues stirring, which was named as Solution A. 526 mg of 2-methylimidazole were added into 40 mL of anhydrous methanol solution with continues stirring until a homogeneous solution formed, which was named as Solution B. Then, Solution A and B were mixed and further added 10 mg of CTAB, the mixture was sonicated for 10 minutes then sealed for 24 h at room temperature. The obtained white ZIF-8 products were washed with anhydrous methanol several times. After drying, the products were transferred to a 40 mL tannic acid solution (0.01 mol L^{-1}), sonicated for 5 min, then collected by centrifugation and washed with water and methanol successively. After drying, the samples were put into a tube furnace and heated at 800 °C for 2 h under N_2 atmosphere. Finally, the collected black powders were immersed in a 1 mol L^{-1} of HCl solution to remove the residual Zn or ZnO. Finally, the samples were dried under vacuum at 100 °C to obtain the final products after washing with deionized water several times. A simple schematic illustration of this process is shown in Figure 1, as follow:

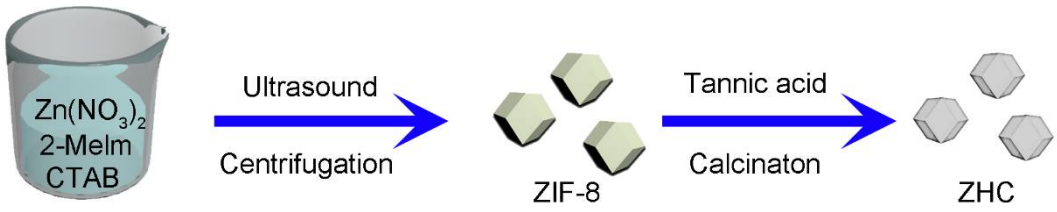

Fig. 1 Schematic illustration of the fabrication process of ZHC.

2.3. Characterization

The microstructure of the material was characterized by scanning electron microscopy (SEM, S-4800). Transmission electron microscopy (TEM) analysis was performed using a JEM-2100F system. The X-ray diffraction (XRD) was carried out with a Cu Kα radiation source (Rigaku). The Brunauer-Emmett-Teller (BET) method was used to provide the specific surface area value. The pore size distribution of the ZHC was obtained from BJH method using DFT method by ASiQwin software[8] (ASAP 2020, Micromeritics, America).

2.4. Adsorption process

The as-prepared ZHC can be applied as an efficient adsorbent for antibiotics in water. The antibiotics solution with increasing concentrations (TC, OFO 5-40 mg L^{-1}, NFO 4-20mg L^{-1}) were carried out in a 100 mL conical flask with 5 mg ZHC; the adsorption begins when the solution is mixed with the absorbent. The adsorption experiments of three antibiotics were carried out at a constant speed (1000 rpm) in order to ensure the uniform diffusion of the absorbent in the solution. The different initial concentrations supernatant solution was obtained by filtering the solution with a syringe through a water filter membrane of 0.22 μm (SHZ - D (Ⅲ) circulating water vacuum pump). After filtering, the supernatant solution for UV−visible spectra was recorded at a characteristic wavelength. A batch of adsorption experiments and blank experiments were conducted under constant temperature and pH values. The maximum adsorption amount of ZHC for TC, OFO and NFO is calculated using the formula (1):

$$q_e = \frac{(c_0 - c_e)m}{V} \qquad (1)$$

where q_e represents the absorption capacity of ZHC, C_0 represents the initial concentration of TC/OFO/NFO, C_e refers to the concentration of TC/OFO/NFO when the solution reaches the adsorption equilibrium, while V represents the solution volume and m represents the mass of the absorbent ZHC.

The adsorption of ZHC for antibiotics is based on Langmuir and Freundlich isothermal adsorption models. The Langmuir model formula [9,10] is as follows:

$$\frac{c_e}{q_e} = \frac{1}{K_L q_m} + \frac{c_e}{q_m} \qquad (2)$$

Where C_e is the equilibrium concentration, K_L is the adsorption constant, and q_m is the maximum adsorption capacity.

The Freundlich model formula [7, 11] is as follows:

$$\ln q_e = \ln K_f + \left(\frac{1}{n}\right) \ln c_e \qquad (2)$$

In the formula, K_f and n representing the Freundlich constant. The higher the value, the better the adsorption effect.

The pseudo-first-order adsorption kinetics model of ZHC for antibiotics assumes that adsorption is controlled by diffusion steps and is given by:[12]

$$\ln(q_e - q_t) = \ln q_e - K_1 t \qquad (3)$$

Where q_t represents the amount of antibiotics absorbed in time t and K_1 represents the first-order kinetic constant.

The pseudo-second-order kinetic model assumes that the adsorption rate is determined by the square value of the number of unoccupied adsorptive vacancies on the adsorbent surface, and the adsorption process is controlled by the chemical adsorption mechanism. The pseudo-second-order kinetic model [12, 13] is as follows:

$$\frac{t}{q_t} = \frac{1}{K_2 {q_e}^2} + \frac{t}{q_e} \qquad (4)$$

In the formula, K_2 represents the pseudo-second-order kinetic constant.

The formula of the intra-particle diffusion model [14, 15] is as follows:

$$q_t = K_{id} t^{1/2} + C \qquad (5)$$

where C is the constant involving the thickness, the boundary layer and K_{id} is the internal diffusion constant. In the particle diffusion model, q_t and $t^{1/2}$ are linearly fitted. If the straight line passes the origin, it is shown that the diffusion of the particles is the rate-limiting step of the

adsorption process, and the adsorption process is controlled by the other adsorption stages if the origin is not passed.

3. Results and discussion

To investigate the crystal structure of obtained ZHC, XRD analysis was conducted. As shown in Fig. 2a, the diffraction peaks (2θ) located at 26.61°, 43.45° and 46.32° can be attributed to the (111), (100), and (110) crystal faces of graphite, respectively; which is in accordance with the peaks displayed in the graphite standard (JCPDS No. 01-075-2078). No impurity peak was found in the XRD pattern, demonstrating the high purity of the obtained ZHC materials. The morphology of ZIF-8 (Fig. S2) and ZHC were explored by SEM. During the synthesis of ZIF-8, the addition of CTAB will significantly reduce the particle size of ZIF-8 crystals. It is speculated that CTAB may control the growth of crystals during synthesis, and the growth control mode may be as follows. Because of the ZIF-8 itself is anisotropic growth, part of CTAB selective adsorption to the lowest on the plane of mutual acting force, when CTAB is added into the precursor solution, CTAB in the process is more likely to act as a capping agent, because CTAB can be absorbed to ZIF-8 crystals on the surface[16-17]. Therefore, the growth and separation of ZIF-8 crystals can be inhibited, and the morphology and size of ZIF-8 nanoparticles can be further controlled. According to the SEM images presented in Fig. 2b and 2c, the particle size of the ZIF material witnessed a slight decrease after carbonization, which can be explained by the shrinkage of organic components during the calcination process. The TEM image displayed in Fig. 2d confirms that the ZHC materials show obvious hollow structures.

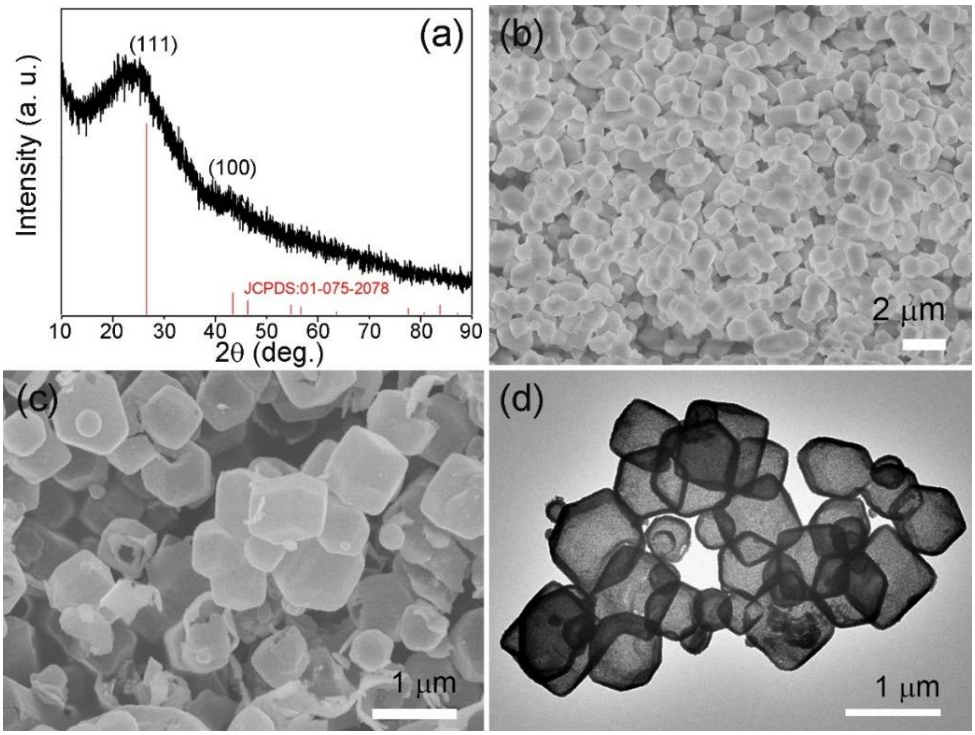

Fig. 2 (a) XRD pattern of the ZHC (b, c) SEM image of ZIF-8 and ZHC (d) TEM image of the obtained ZHC.

N_2 adsorption-desorption isotherms were carried out to investigate the pore diameter distribution and the specific surface area of ZHC. It can be seen from Fig. 3a that the relative pressure (P/P_0) between 0.2-0.9 shows a gradual upward trend of nitrogen adsorption and the pore diameter is concentrated at 5 nm (Fig. 3b), which indicates that a mesoporous structure exists in the ZHC material. The adsorbent with high surface area (807.56 $m^2 g^{-1}$) can enhance the adsorption capacity of the adsorbent due to its abundant active adsorption sites. In addition, the mesoporous structure always gives rise to the ability and efficiency of removing antibiotics pollutants.

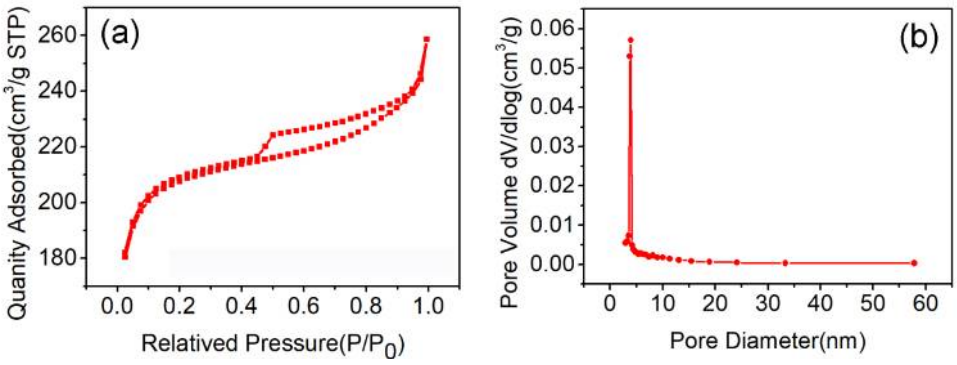

Fig. 3 (a) N_2 adsorption-desorption isotherm, and (b) pore size distribution of ZHC (N_2 77K, DFT).

According to the data in Table 1, the adsorption process of the ZHC on TC, NFO and OFO are in accordance with the Langmuir (Fig. 4a, b) and Freundlich (Fig. 4c, d) models. However, considering the correlation fitting coefficient, the Langmuir model can describe the adsorption process well; that is, the adsorption of the material on TC, NFO and OFO is homogeneous in the single molecular layer. Fitting of experimental data to model equations based on the Langmuir model show the adsorption capacity of the ZHC on TC, NFO and OFO are 267.3, 125.6 and 227.8 mg g^{-1}, respectively.

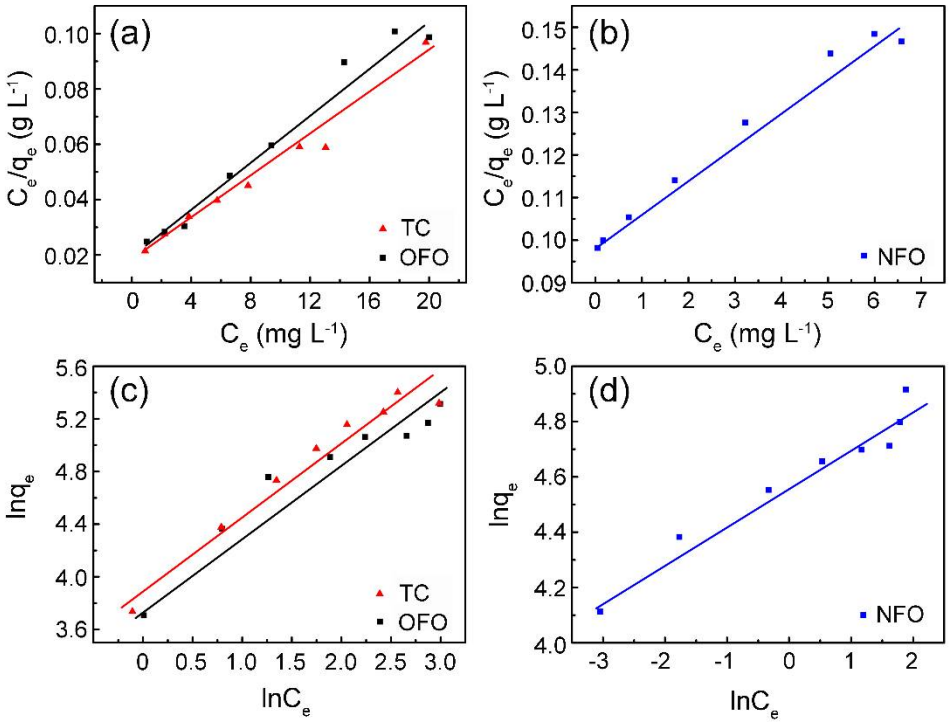

Fig. 4 The isothermal adsorption fitting curves of Langmuir (a, b) and Freundlich (c, d) for TC, OFO and NFO by ZHC.

Table 1 The relevant fitting parameters of TC, NFO and OFO simulated using Langmuir and Freundlich models.

Pollutants	Langmuir			Freundlich		
	K_L (L mg^{-1})	q_m (mg g^{-1})	R^2	K_f (mg g^{-1}) (L mg^{-1})$^{1/n}$	n	R^2
TC	0.212	267.3	0.972	70.80	1.8319	0.948
NFO	0.079	125.6	0.979	53.41	7.23	0.945
OFO	0.230	227.8	0.973	26.08	2.114	0.91

As can be found in Table 2, the ZHC exhibits much higher antibiotics adsorption ability than pure ZIF-8 (Fig. S3) and that of several inorganic materials in the reported literature, demonstrating the huge potential of the ZHC in adsorption applications.

Table 2 Comparison of the TC, NFO and OFO adsorption ability of ZHC with other inorganic adsorbents.

Antibiotics	Adsorbents	q_m (mg g^{-1})	Condition (pH)	Reference
Tetracycline	GN	2 x 10^{-4}	7	[18]
	E_3D_7	133.3	8	[19]
	CNT-2%O	217.8	4	[20]
	Biochar	102	6	[21]
	ZIF-8	119.04	7	This work
	ZHC	267.3	7	This work
Norfloxacin	RGOS	50	6	[22]
	H-CNTS	76.3	7	[23]
	ZIF-8	38.69	7	This work
	ZHC	125.6	7	This work
Ofloxacin	GN	0.2	7	[18]
	BEPS-free biofilm-50	5.27	7	[24]
	Cassava residue-derived biochar	3.00	7	[25]
	ZIF-8	111.48	7	This work
	ZHC	227.8	7	This work

Fig. 5a shows that the adsorption of the ZHC to the three antibiotics reached equilibrium after ~ 48 h. Fig. 5b and Fig. 5c are the fitted curves of pseudo-first-order dynamic models and pseudo-second-order dynamic models, respectively. Considering the correlation coefficient R^2 values in Table 3, it can be concluded that the adsorption of the ZHC to the three antibiotics is more in line with the pseudo-second-order kinetic model, meaning chemical adsorption mechanism exists in the adsorption process[7]. Fig. 5d depicts the fitting curve of intra-particle diffusion model, which indicates that the adsorption process of antibiotics can be divided into three stages: (1) antibiotics diffuse on the surface of the adsorbent, (2) antibiotics penetrate in the inner structure of ZHC through pores, (3) antibiotics interact with the surface-active sites of ZHC.

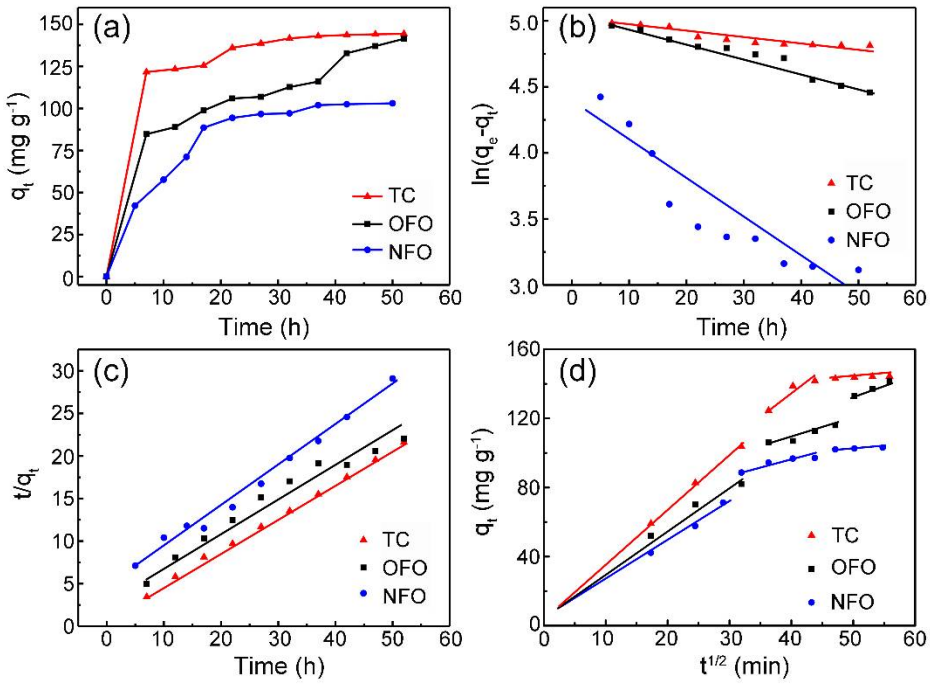

Fig. 5 (a) Time curve fitting, (b) pseudo-first-order kinetic model, (c) pseudo-second-order kinetic model, and (d) the intra-particle diffusion model of ZHC.

Table 3 The related fitting parameters of the kinetic model.

Model	C_0 (mg L^{-1})	Pseudo-first-order K_1 (L min^{-1})	Pseudo-first-order $q_{e,cal}$ (mg g^{-1})	Pseudo-first-order R^2	Pseudo-second-order K_2 (g $mg^{-1}min^{-1}$)	Pseudo-second-order $q_{e,cal}$ (mg g^{-1})	Pseudo-second-order R^2
TC	40	0.00422	148.21	0.852	4.33×10^{-5}	151.89	0.998
NFO	20	0.02963	76.77	0.87	6.25×10^{-5}	126.17	0.987
OFO	40	0.01136	158.92	0.954	3.83×10^{-5}	161.60	0.961

4. Conclusions

In summary, a novel ZIF-8 derived hollow carbon (ZHC) was developed as efficient adsorbents to remove the residual antibiotics in the polluted water. The strong adsorption capacity was confirmed by Langmuir and Freundlich isothermal adsorption experiments, dynamic analysis as well as theoretical calculation. The maximum quantities of ZHC on adsorbing tetracycline (TC), norfloxacin (NFO) and levofloxacin (OFO) are 267.3, 125.6 and 227.8 mg g^{-1}, respectively. The excellent adsorptive performance of ZHC could be attributed to the hollow structure, which endows its high BET surface area and sufficient adsorption sites. Our results suggested that the MOF derived carbon-material provides an extensible method to efficiently remove the antibiotics in the environment.

Acknowledgements: The work has been funded by the National Natural Science Foundation of China (51602193, 21601122, 51701022), Shanghai "Chen Guang" project (16CG63), the Fundamental Research Funds for the Central Universities (WD1817002), and the Talent Program of Shanghai University of Engineering Science, Science and Technology Facilities Council for STFC/MDC Futures Early Career Award, and Engineering and Physical Sciences Research Council (EPSRC) (EP/R023581/1)

REFERENCES

1 Michael, I.; Rizzo, L.; McArdell, C. S.; Manaia, C. M.; Merlin, C.; Schwartz, T.; Dagot, C.; Fatta-Kassinos, D. Urban wastewater treatment plants as hotspots for the release of antibiotics in the environment: A review, *Water Res*, **2013**, 47, 957-995.

2 Liu, M.K.; Liu, Y.Y.; Bao, D.D.; Zhu, G.; Yang, G.H.; Geng J.F.; Li, H.T. Effective Removal of Tetracycline Antibiotics from Water using Hybrid Carbon Membranes, *Sci Rep-UK*, **2017**, *7*, 43717.

3 Zhou, H.C.; Long J.R.; Yaghi, O.M. Introduction to Metal-Organic Frameworks, *Chem Rev*, **2012**, *112*, 673-674.

4 Chaikittisilp, W.; Ariga, K.; Yamauchi, Y. A new family of carbon materials: synthesis of MOF-derived nanoporous carbons and their promising applications, *J Mater Chem A*, **2013**, *1*, 14-19.

5 Xu, H.; Zhou, S.; Xiao, L.; Wang, H.; Li S.; Yuan, Q. Fabrication of a nitrogen-doped graphene quantum dot from MOF-derived porous carbon and its application for highly selective fluorescence detection of Fe^{3+}, *J Mater Chem C*, **2015**, *3*, 291-297.

6 Pachfule, P.; Shinde, D.; Majumder M.; Xu, Q. Fabrication of carbon nanorods and graphene nanoribbons from a metal-organic framework, *Nat Chem*, **2016**, *8*, 718-724.

7 Xia, W.; Qiu, B.; Xia D.; Zou, R. Facile preparation of hierarchically porous carbons from metal-organic gels and their application in energy storage, *Sci Rep-UK*, **2013**, *3*, 1935.

8 Zhou, N.; Du, Y.; Wang, C.; Chen, R. Facile synthesis of hierarchically porous carbons by controlling the initial oxygen concentration in-situ carbonization of ZIF-8 for efficient water treatment, *Chinese J Chem Eng*, **2018**, 10.1016/j.cjche.2018.05.014.

9 Li, W.; Wang, J.; He, G.; Yu, L.; Noor, N.; Sun, N.; Zhou, X.; Hu J.; Parkin, I.P. Enhanced adsorption capacity of ultralong hydrogen titanate nanobelts for antibiotics, *J Mater Chem A*, **2017**, *5*, 4352-4358.

10 I. Langmuir, The adsorption of gases on plane surfaces of glass, mica and platinum, *J. Am. Chem. Soc.* **1918**, *40*, 1361-1403.

11 H.M.F. Freundlich, Over the adsorption in solution, J. Phys. Chem., **1906**, *57*, 385-470.

12 Dai, J.; Xiao, X.; Duan, S.; Liu, J.; He, J.; Lei, J.; Wang, L. Synthesis of novel microporous nanocomposites of ZIF-8 on multiwalled carbon nanotubes for adsorptive removing benzoic acid from water, *Chem Eng J*, **2018**, *331*, 64-74.

13 Y.-S. Ho, Review of second-order models for adsorption systems, *J. Hazard. Mater.*, **2006**, *136*, 681-689.

14 Singh, S. K.; Townsend, T.G.; Mazyck D.; Boyer, T.H. Equilibrium and intra-particle diffusion of stabilized landfill leachate onto micro- and meso-porous activated carbon, *Water Res*, **2012**, *46*, 491-499.

15 Liu, Q.; Zhong, L.; Zhao, Q.; Frear, C.; Zheng Y. Synthesis of Fe_3O_4/Polyacrylonitrile Composite Electrospun Nanofiber Mat for Effective Adsorption of Tetracycline, *ACS Appl. Mater. Interfaces*, **2015**, 7, 14573-14583.

16 Hsu, S.H.; Li, C.T.; Chien, H.T.; Salunkhe, R.R.; Suzuki, N.; Yamauchi, Y.; Ho K.C.; Wu, K.C.W. Platinum-Free Counter Electrode Comprised of Metal-Organic-Framework (MOF)-Derived Cobalt Sulfide Nanoparticles for Efficient Dye-Sensitized Solar Cells (DSSCs), *Sci Rep-UK*, **2014**, *4*, 6983.

17 Zhao, H.; Wang Y.; Zhao, L. Magnetic Nanocomposites Derived from Hollow ZIF-67 and Core-Shell ZIF-67@ZIF-8: Synthesis, Properties, and Adsorption of Rhodamine B, *Eur J Inorg Chem*, **2017**, *35*, 4110-4116.

18 Peng, B.; Chen, L.; Que, C.; Yang, K.; Deng, F.; Deng, X.; Shi, G.; Xu G.; Wu, M. Adsorption of Antibiotics on Graphene and Biochar in Aqueous Solutions Induced by pi-pi Interactions, *Sci Rep-UK*, **2016**, *6*, 31920.

19 Zhu, Z.; Zhang, M.; Wang, W.; Zhou Q.; Liu, F. Efficient and synergistic removal of tetracycline and Cu(II) using novel magnetic multi-amine resins, *Sci Rep-UK*, **2018**, *8*, 4762.

20 Yu, F.; Ma J.; Han, S. Adsorption of tetracycline from aqueous solutions onto multi-walled carbon nanotubes with different oxygen contents, *Sci Rep-UK*, **2014**, *4*, 5326.

21 Zhou, Y.; Liu, X. Modification of biochar derived from sawdust and its application in removal of tetracycline and copper from aqueous solution: Adsorption mechanism and modelling, *Bioresour Technol*, **2017**, *245*, 266-273.

22 Zhang, X.; Shen, J.; Zhuo, N.; Tian, Z.; Xu, P.; Yang Z.; Yang, W. Interactions between Antibiotics and Graphene-Based Materials in Water: A Comparative Experimental and Theoretical Investigation, *ACS Appl Mater Inter*, **2016**, *8*, 24273-24280.

23 Wang, Z.; Yu, X.; Pan B.; Xing, B. Norfloxacin Sorption and Its Thermodynamics on Surface-Modified Carbon Nanotubes, *Environ Sci Technol*, **2010**, *44*, 978-984.

24 Zhang, L.; Dong, D.; Hua X.; Guo, Z. Inhibitory effects of extracellular polymeric substances on ofloxacin sorption by natural biofilms, *Sci Total Environ*, **2018**, *625*, 178-184.

25 Huang, P.; Ge, C.; Feng, D. Effects of metal ions and pH on ofloxacin sorption to cassava residue-derived biochar, *Sci Total Environ*, **2018**, *616-617*, 1384-1391.